Nucleic Acids Research, 2018 **1**
doi: 10.1093/nar/gky603

The primary transcriptome, small RNAs and regulation of antimicrobial resistance in *Acinetobacter baumannii* ATCC 17978

Carsten Kröger[1,*], Keith D. MacKenzie[2,3], Ebtihal Y. Alshabib[2,3], Morgan W. B. Kirzinger[2], Danae M. Suchan[2,3], Tzu-Chiao Chao[3,4], Valentyna Akulova[2], Aleksandra A. Miranda-CasoLuengo[1], Vivian A. Monzon[1], Tyrrell Conway[5], Sathesh K. Sivasankaran[6], Jay C. D. Hinton[7], Karsten Hokamp[8] and Andrew D. S. Cameron[2,3,*]

[1]Department of Microbiology, School of Genetics & Microbiology, Moyne Institute of Preventive Medicine, Trinity College Dublin, Dublin 2, Ireland, [2]Institute for Microbial Systems and Society, University of Regina, Regina, Saskatchewan S4S 0A2, Canada, [3]Department of Biology, University of Regina, Regina, Saskatchewan S4S 0A2, Canada, [4]Institute of Environmental Change and Society, University of Regina, Regina, Saskatchewan S4S 0A2, Canada, [5]Department of Microbiology and Molecular Genetics, Oklahoma State University, Stillwater, OK 74078, USA, [6]John P. Hussman Institute for Human Genomics, Miller School of Medicine, University of Miami, Miami, FL, USA, [7]Institute of Integrative Biology, University of Liverpool, Liverpool L69 7ZB, UK and [8]Department of Genetics, School of Genetics & Microbiology, Smurfit Institute of Genetics, Trinity College Dublin, Dublin 2, Ireland

Received December 20, 2017; Revised June 21, 2018; Editorial Decision June 24, 2018; Accepted June 26, 2018

ABSTRACT

We present the first high-resolution determination of transcriptome architecture in the priority pathogen *Acinetobacter baumannii*. Pooled RNA from 16 laboratory conditions was used for differential RNA-seq (dRNA-seq) to identify 3731 transcriptional start sites (TSS) and 110 small RNAs, including the first identification in *A. baumannii* of sRNAs encoded at the 3′ end of coding genes. Most sRNAs were conserved among sequenced *A. baumannii* genomes, but were only weakly conserved or absent in other *Acinetobacter* species. Single nucleotide mapping of TSS enabled prediction of −10 and −35 RNA polymerase binding sites and revealed an unprecedented base preference at position +2 that hints at an unrecognized transcriptional regulatory mechanism. To apply functional genomics to the problem of antimicrobial resistance, we dissected the transcriptional regulation of the drug efflux pump responsible for chloramphenicol resistance, *craA*. The two *craA* promoters were both down-regulated >1000-fold when cells were shifted to nutrient limited medium. This conditional down-regulation of *craA* expression renders cells sensitive to chloramphenicol, a highly effective antibiotic for the treatment of multidrug resistant infections. An online interface that facilitates open data access and visualization is provided as 'AcinetoCom' (http://bioinf.gen.tcd.ie/acinetocom/).

INTRODUCTION

In 2017, the World Health Organization (WHO) ranked carbapenem-resistant *Acinetobacter baumannii* as the top priority critical pathogen in the WHO's first-ever list of priority antimicrobial-resistant pathogens (1,2). It is estimated that one million *A. baumannii* infections occur worldwide each year, causing 15 000 deaths (3). In the United States, *A. baumannii* is responsible for more than 10% of nosocomial infections, and causes a variety of diseases such as ventilator-associated pneumonia, bacteraemia, skin and soft tissue infections, endocarditis, urinary tract infections and meningitis (4). Despite the urgency to develop new antimicrobial drugs, we know little about *A. baumannii* infection biology and virulence mechanisms because only a few *A. baumannii* virulence genes and their regulation have been functionally studied (5).

Characterizing the transcriptional landscape and simultaneously quantifying gene expression on a genome-wide scale using RNA sequencing (RNA-seq) is a cornerstone of functional genomic efforts to identify the genetic basis of cellular processes (6). RNA-seq identifies transcripts for an entire genome at single-nucleotide resolution in a strand-specific fashion, making it an ideal tool to un-

*To whom correspondence should be addressed. Tel. +353 1 896 1414; Email: Carsten.Kroeger@tcd.ie
Correspondence may also be addressed to Andrew D.S. Cameron. Tel. +1 306 337 2568; Email: Andrew.Cameron@uregina.ca

cover transcriptome features. Recent technical enhancements to RNA-seq enable improved delineation of transcriptional units to localize TSS, transcript ends, sRNAs, antisense transcription and other transcriptome features (6,7). The ability to quantify gene expression and characterize transcripts from any organism is particularly valuable for the study of emerging bacterial pathogens, where research knowledge lags behind the global spread, health burden and economic impacts of disease.

To address the lack of basic biological insight of *A. baumannii*, we used a functional genomics approach to investigate the transcriptome architecture of *A. baumannii* ATCC 17978 and to investigate virulence and antibiotic resistance gene expression in this priority pathogen. *A. baumannii* ATCC 17978 is one of the best-studied strains of *Acinetobacter*, and is a useful model for genetic manipulation due to its natural sensitivity to most antibiotics used in the laboratory (8,9). Differential RNA-seq (dRNA-seq) facilitates the precise identification of TSS by distinguishing 5′ triphosphorylated (i.e. newly synthesized, 'primary' transcripts from the dephosphorylated 5′ termini) of processed RNA species (10). dRNA-seq analysis of transcription in virulence-relevant conditions, antimicrobial challenge, and standard laboratory culture generated a high-resolution map of TSS and small RNAs in the *A. baumannii* chromosome, revealing the precise location of 3731 promoters and 110 small RNAs. This comprehensive view of TSS identified two promoters that regulate chloramphenicol resistance by the CraA efflux pump and we discovered growth conditions that stimulate low *craA* expression and render *A. baumannii* sensitive to chloramphenicol. To facilitate similar discoveries by the research community, we created the online resource AcinetoCom (http://bioinf.gen.tcd.ie/acinetocom/) for free and intuitive exploration of the *A. baumannii* ATCC 17978 transcriptome.

MATERIALS AND METHODS

Bacterial strains and growth conditions

Acinetobacter baumannii ATCC 17978 was obtained from LGC-Standards-ATCC. We used the reference strain containing all three plasmids (pAB1, pAB2, pAB3) for dRNA-seq analysis. Cells were cultured overnight in 5 ml Lennox (L-) broth (10 g l^{-1} tryptone, 5 g l^{-1} yeast extract, 5 g l^{-1} NaCl; pH 7.0). For routine cultures, cells were sub-cultured (1:1000) in 250-ml flasks containing 25 ml of growth medium and grown with shaking at 220 RPM in a waterbath. For experiments in non-standard conditions or when exposing cells to specific challenges, a fresh L-broth culture was grown for 2–3 h to achieve steady-state exponential growth physiology before inoculation into an alternate growth condition or challenge.

To maximize the number of TSS identified, cells were exposed to a diversity of growth conditions (detailed below) to induce expression from as many gene promoters as possible. RNA extracts from cells in each of 16 conditions were pooled together into a single sample, creating the 'Pool' sample summarized in Table 1. To capture all TSS in the different growth stages of routine L-broth culture, cells were grown in L-broth at 37°C and sampled at select culture densities (OD_{600} values of 0.25, 0.75, 1.8, 2.5 and 2.8). To identify TSS expressed in the presence of disinfectants and antimicrobial agents, L-broth cultures of exponentially-growing cells (OD_{600} of 0.3) at 37°C were subjected to 10-min shocks, containing either a 1:100,000 dilution of disinfectant (Distel 'High Level Medical Surface Disinfectant', non-fragranced), hydrogen peroxide to a final concentration of 1 mM, ethanol to a final concentration (v/v) of 2%, kanamycin to a final concentration of 50 μg ml^{-1}, NaCl to a final concentration of 0.3 M or 2,2′-dipyridyl to a final concentration of 0.2 mM. To mimic growth in environmental conditions, cells were cultured in L-broth at low temperatures (25°C) until an OD_{600} of 0.3; these same cultures were transferred to 37°C for 10 min. To evaluate gene expression in response to alternative nutrient environments, overnight cell cultures were sub-cultured in liquid M9 minimal medium supplemented with 1 mM $MgSO_4$, 0.1 mM $CaCl_2$ and a carbon source of either 31.2 mM fumarate or 33.3 mM xylose, and grown at 37°C to an OD_{600} of 0.3. For growth on solid media, *A. baumannii* 17978 was plated on L-agar plates and grown for 16 hours at 37°C.

Acinetobacter baumannii ATCC 17978 was also used for early stationary phase (ESP) transcriptome analysis via RNA-seq. For this analysis, cells were sub-cultured in 250 ml flasks containing 25 ml of L-broth and grown with shaking at 37°C to an OD_{600} of 2.0. RNA-seq revealed that pAB3 was absent in the strain used for this analysis, indicating that pAB3 was lost during shipping of ATCC 17978 between our laboratories. A comparison of RNA-seq reads to the reference genome did not detect any point mutations in the derivative strain lacking pAB3.

RNA extraction, ribosomal RNA depletion, DNase digestion and the RNA pool

Total RNA was isolated from cultures of *A. baumannii* ATCC 17978 cells using TRIzol as described previously for *Salmonella enterica* serovar Typhimurium (11). The RNA quality was analyzed using an Agilent Bioanalyzer 2100 and RNA concentration was measured on a NanoDrop™ spectrophotometer or the Qubit™ (Invitrogen). To generate the pooled RNA sample for dRNA-seq analysis, equal amounts of RNA from each growth condition were combined into a single sample. For ESP transcriptome analysis, three biological replicates were generated. These ESP samples were depleted for ribosomal RNA using the RiboZero rRNA Removal Kit Bacteria (Illumina). Contaminating DNA was removed from ESP and pooled RNA samples via DNase I (TURBO DNA-free™ kit, Ambion) digestion; the pooled RNA sample was also DNase I treated (TURBO DNase I, Ambion) as part of sample workflow by vertis Biotechnologie AG (Freising, Germany).

Library preparation for next generation sequencing

The pooled RNA sample was divided into two separate aliquots prior to library preparation. Libraries of both aliquots were prepared by vertis Biotechnologie AG (Freising, Germany) and sequenced on an Illumina NextSeq machine (single reads). For dRNA-seq, one of the two aliquots were digested with Terminator Exonuclease (TEX) prior to cDNA library preparation (10,12). Libraries of the ESP

Table 1. Growth conditions used to induce the global *A. baumannii* transcriptome

Condition name	Growth description
OD 0.25	Growth in Lennox broth to OD600 0.25
OD 0.75	Growth in Lennox broth to OD600 0.75
OD 1.8	Growth in Lennox broth to OD600 1.8
OD 2.5	Growth in Lennox broth to OD600 2.5
OD 2.8	Growth in Lennox broth to OD600 2.8
25°C	Growth in Lennox broth to OD600 0.3 at 25°C.
Temp10	Growth in Lennox broth to OD600 0.3 at 25°C; then transfer to 37°C for 10 min.
NaCl shock	Growth in Lennox broth to OD600 0.3; then addition of NaCl (Sigma, Cat. S3014) to a final concentration of 0.3 M for 10 min.
LowFe^{2+} shock	Growth in Lennox broth to OD600 0.3; then addition of 2,2′-dipyridyl (Sigma, Cat. D21630) to a final concentration of 0.2 mM for 10 min.
H_2O_2 shock	Growth in Lennox broth to OD600 0.3; then addition of H_2O_2 (Merck, Cat. 822287) to final concentration of 1 mM H_2O_2 for 10 min.
Kan shock	Growth in Lennox broth to OD600 0.3; then addition of kanamycin to final concentration of 50 μg/ml for 10 min.
EtOH shock	Growth in Lennox broth to OD600 0.3; then addition of ethanol to final concentration of 2% (v/v) for 10 min.
Disinf shock	Growth in Lennox broth to OD600 0.3; then addition of 250 μl disinfectant Distel 'High Level Medical Surface Disinfectant', non-fragranced (1:100 dilution, VWR, Cat. 141-0933) for (1:100 dilution) for 10 min
L-agar	Growth on an Lennox broth agar plate for 16 h at 37°C
M9+xyl	Growth in M9 minimal medium (incl. 1 mM $MgSO_4$, 0.1 uM $CaCl_2$, 33.3 mM D-xylose (Sigma, Cat. X3877) to OD600 0.3)
M9+fum	Growth in M9 minimal medium (incl. 1 mM $MgSO_4$, 0.1 uM $CaCl_2$, 31.2 mM sodium fumarate (Sigma, Cat. F1506) to OD600 0.3)
ESP	Growth in Lennox broth to OD_{600} 2.0

RNA samples were prepared using the NEBNext™ Ultra RNA Library Prep Kit for Illumina (NEB) according to the manufacturer's instructions. These libraries were sequenced on an Illumina MiSeq (paired-end reads). We noted that for very highly-expressed genes in the ESP samples, there were distinct transcripts mapped to the opposite strand that perfectly mirrored the expected transcript. This is best explained by incomplete depletion of non-template strand (second strand incorporated dUTP) by the USER enzyme during library preparation with NEBNext™ Ultra. Therefore, we considered only the pooled RNA-seq data from vertis Biotechnologie AG, which is generated by an RNA adaptor ligation step before cDNA synthesis, to determine the amount of antisense transcription.

Mapping of sequencing reads, statistics and analysis

The original genome sequence for *A. baumannii* ATCC 17978 identified two plasmids (pAB1 and pAB2) (8). However, it was subsequently revealed that ATCC 17978 carries a third plasmid (pAB3) that was incorrectly assembled as chromosome sequence in the first assembly (13), thus the *A. baumannii* ATCC 17978-mff genome (accession: NZ_CP012004.1) was used as a reference sequence in our study. Quality control was carried out using FastQC and showed excellent quality for the sequencing data. DNA sequencing reads were mapped using bowtie2 with the –very-sensitive –local settings for use of soft-clipping and maximum sensitivity (14). Conversion into BAM and BigWig files was carried out using SAMtools (15) and Galaxy at galaxy.org (16). Mapped reads were visualized in the Integrated Genome Browser (IGB) (17) and Jbrowse (18). Number of sequence reads mapped were (the underscore indicates the biological replicate) ESP_1 (10,588,403; mapped uniquely: 8,403,658), ESP_2 (9,374,114; mapped uniquely: 6,769,516), ESP_3 (11,121,847; mapped uniquely: 7,891,371, RNA_pool (66,853,984: mapped uniquely: 19,607,931) and dRNA-seq_Pool (77,237,102; mapped uniquely: 30,041,320). The difference in percentage of uniquely mapped reads of the ESP conditions and the Pool samples is caused by the fact that RNA from the ESP condition was depleted for rRNA, while the RNA samples of the RNA Pool were not. FeatureCounts was used to summarize read counts for each annotated feature (19). These values were transformed into transcripts per million reads (TPM) following the formula provided by Li *et al.* (20); (Supplementary Table S4).

Identification and categorization of TSS

Before the identification of TSS, the coverage files for the RNA Pool and TEX-digested RNA Pool sample were normalized to account for different library sizes in the following way: the number of mapped nucleotides for each position was divided by the number of uniquely mapped reads of the smallest library (ESP_2) and then multiplied by the number of reads for the library being normalized. The locations of TSS were predicted with TSSpredator (21), which is used to assess enrichment of reads in the TEX-digested sample over the non-TEX-digested control; enrichment is reflective of a 5′ triphosphate protecting the transcript from TEX digestion. Default settings were used, with the exception of changing the step height option to 0.2, the 5′ UTR (untranslated region) length to 400 and the enrichment factor to 1.5. The locations of the predicted TSS were manually inspected in IGB and Jbrowse. TSS that exist ≤400 nt upstream of the start of a coding region and TSS of non-coding RNA genes were classified as Primary or Secondary TSS; in cases where multiple candidate TSS are upstream, the TSS associated with the strongest expression was designated as the Primary TSS, while all additional TSS were designated Secondary TSS. TSS with intragenic location on the sense strand were classified as Internal TSS and when located on the antisense strand as Antisense TSS. TSS were

classified as Orphan if they could not be assigned to any other category. Occasionally, manual curation changed the classification of TSS, e.g. five genes with a 5′ UTR >400 nt were classified as Primary or Secondary (Supplementary Table S2).

Rapid amplification of cDNA ends (5′ RACE)

5′ RACE experiments were carried out as described earlier (11,22) with the following modifications: Twenty-four μg of DNaseI-treated total RNA isolated from *A. baumannii* cells grown in L-broth to ESP was split into two 12 μg aliquots of which one was treated with 10 U pyrophosphohydrolase RppH (NEB). The other aliquot remained untreated as a negative control. Following phenol-chloroform extraction and sodium-acetate precipitation, a single strand RNA oligonucleotide was ligated to the RNA samples using single strand RNA ligase (NEB). Following phenol–chloroform extraction and Na-acetate precipitation, two μg of linker-ligated RNA (RppH- and mock-treated) was used to synthesize cDNA using random hexamer priming and Superscript III reverse transcriptase (Invitrogen). Taq polymerase was used for PCR amplification of RACE products to facilitate cloning and sequencing of RACE products using the TOPO cloning vector pCR2.1 (Invitrogen). After transformation of *Escherichia coli* TOPO cells with pCR2.1 containing RACE products, plasmid DNA of five clones was isolated and inserts sequenced. All five sequences agreed with the TSS identified by dRNA-seq. Oligonucleotides used are listed in Supplementary Table S1.

Identification of −10 and −35 sigma factor motifs

DNA sequences upstream of all transcription start sites were extracted in two blocks of nucleotides: between position −3 to −18 (−10 block) and between −16 to −50 (−35 block). Each block was searched with the unbiased motif finding program MEME 4.11.2 (23). Each sequence block was searched with the following settings: one occurrence per sequence with a width of 6–12 bp (−10 motif) or 4–10 bp (−35 motif). Sequence logos were generated by WebLogo (24).

Identification of candidate sRNA genes and prediction of transcription terminators

The identification of candidate sRNA genes was carried out by searching mapped sequence reads in IGB and Jbrowse for short unannotated transcripts as well as by using the output from the TSSpredator software, which annotates orphan and internal TSS that may represent new sRNA candidates. A new candidate sRNA gene was assigned if a short (<500 nt) unannotated transcript was observed in the RNA-seq data. A minimum cutoff for expression was set at TPM > 10, as previously described (12). The borders of the transcript were informed by the location of TSS determined by dRNA-seq data and the location of predicted Rho-independent transcription terminators using ARNold with the default setting (25).

sRNA conservation analysis

The conservation of candidate sRNA genes was investigated using GLSEARCH (26). The genome sequences were obtained from NCBI (*A. baumannii* Ab04-mff (NZ_CP012006.1), *A. baumannii* AB030 (NZ_CP009257.1), *A. baumannii* AB0057 (NC_011586.1), *A. baumannii* AB5075-UW (NZ_CP008706.1), *A. baumannii* ACICU (NC_010611.1), *A. baumannii* strain ATCC 17978 (NZ_CP018664.1), *A. baumannii* ATCC 17978-mff (NZ_CP012004.1), *A. baumannii* str. AYE (NC_010410.1), *A. baumannii* IOMTU 433 (NZ_AP014649.1), *A. baumannii* LAC-4 (NZ_CP007712.1), *A. baumannii* A1 (NZ_CP010781.1), *A. baumannii* USA15 (NZ_CP020595.1), *A. baumannii* XH386 (NZ_CP010779.1), *A. baumannii* TYTH-1 (NC_018706.1), *A. baumannii* XDR-BJ83 (NZ_CP018421.1), *Acinetobacter baylyi* DSM 14961 (NZ_KB849622.1-NZ_KB849630.1), *Acinetobacter equi* 114 (NZ_CP012808.1), *Acinetobacter haemolyticus* CIP 64.3 (NZ_KB849798.1-KB849812.1), *Acinetobacter lwoffii* NCTC 5866 (NZ_KB851224.1-NZ_KB851239.1), *Acinetobacter nosocomialis* 6411 (NZ_CP010368.1), *Acinetobacter pittii* PHEA-2 (NC_016603.1), *Acinetobacter venetianus* VE-C3 (NZ_CM001772.1), *Moraxella catarrhalis* BBH18 (NC_014147.1), *Pseudomonas aeruginosa* PAO1 (NC_002516.2), *Pseudomonas fluorescens* F113 (NC_016830.1), *Pseudomonas putida* KT2440 (NC_002947.4), *Pseudomonas syringae* pv. *syringae* B728a (NC_007005.1). The score shows percentage sequence identity with the reference sequence (*A. baumannii* 17978-mff).

Northern blotting

Northern blotting was performed using the DIG Northern Starter Kit (Roche) using DIG-labelled riboprobes generated by *in vitro* transcription as described earlier and according to the manufacturer's instructions (11). Templates for *in vitro* transcriptions using T7 RNA polymerase were generated by PCR using DNA oligonucleotides listed in Supplementary Table S1. Five microgram of total RNA was separated on a 7% urea–polyacrylamide gel in 1× Tris-borate-EDTA (TBE) buffer cooled to 4°C. Band sizes on the northern blots were compared with Low Range single strand RNA ladder (NEB). After blotting and UV crosslinking, the lane with the ladder was cut off, stained with 0.1% methylene blue solution for 1 min at room temperature, destained in sterile water, and re-attached to the membrane before detection of chemiluminescent bands using an ImageQuant LAS4000 imager (GE Healthcare).

Chloramphenicol sensitivity and *craA* expression analysis

Cells were cultured overnight in L-broth containing 25 μg ml^{-1} chloramphenicol and the next morning inoculated to OD_{600} 0.05 in 20 ml fresh medium and grown to OD_{600} of 0.3 in a 250-ml flask with shaking at 37°C. Cells were captured on 0.2 μm analytical test filter funnels (Nalgene), washed with M9 containing 20 mM pyruvate as the carbon source and the filter (retaining the cells) was transferred to M9 plus pyruvate. The cells were washed off the filter and inoculated in fresh 20 mL M9 plus pyruvate medium at

an OD_{600} of 0.1 and incubated at 37°C with shaking for 5 days. Sampling for qPCR and chloramphenicol resistance was performed at $t = 0$, 4, 24, 48 and 96 h and transcription was stopped by the addition of phenol:ethanol stop solution (27,28). For qPCR, total RNA was isolated from cultures using the EZ-10 Spin Column Total RNA Mini-Preps Super Kit (BioBasic) and purity and quality was assessed by 1% agarose gel electrophoresis. For each sample, 5 μg total RNA was DNase treated in a 50 μl reaction using the TURBO DNA-free kit (AMBION), and cDNA templates were synthesized by random priming 0.5 μg RNA in a 20 μl reaction using Verso cDNA synthesis kit (Fisher). PCR reactions were carried out in duplicate with each primer set on an ABI StepOnePlus PCR System (Applied Biosystems) using Perfecta SYBR Fastmix with ROX (Quanta Biosciences). Standard curves were included in every qPCR run; standard curves were generated for each primer set using five serial ten-fold dilutions of *A. baumannii* genomic DNA. Quantitative PCR (qPCR) primers are listed in Supplementary Table S1. Viable counts were performed by serial dilution and drop-plating on L-agar plates without or with chloramphenicol (10 μg ml^{-1}); colony forming units were counted after overnight incubation at 37°C.

RESULTS AND DISCUSSION

Global identification of *A. baumannii* TSS

To generate a comprehensive list of TSS for *A. baumannii* ATCC 17978, we adopted the technique developed for *Salmonella* Typhimurium in which diverse laboratory conditions were used to elicit transcription activation from as many gene promoters as possible (12). Thus, we used 16 conditions that reflect a diversity of environments experienced by *A. baumannii* during infection, environmental survival, and general stress (Table 1). Specifically, *A. baumannii* was cultured in L-broth and sampled throughout growth at OD_{600} 0.25, 0.75, 1.8, 2.5, 2.8, in liquid M9 minimal medium with different sole carbon sources (xylose, fumarate), and grown on an L-agar plate for 16 h at 37°C, and in liquid L-broth at OD_{600} 0.3 at 25°C. These conditions encompass high nutrient (L-broth) and low nutrient (M9) conditions; amino acids (L-broth) and carbohydrates (M9) as primary carbon sources; solid (L-agar) and liquid media; host (37°C) and external (25°C); and a full range of growth states, including stages of rapid growth in which bulk transcription rates are very high, to stationary phase in both rich and energy poor media, when transcriptional output is low and favors long-lived transcripts (29). We also isolated RNA from several 'shock' conditions, including disinfectant shock, osmotic shock (addition of sodium chloride), limitation of iron availability (addition of 2,2′-dipyridyl), translational stress (addition of kanamycin), oxidative stress (addition of hydrogen peroxide), temperature shift from ambient to body temperature (25–37°C), and the addition of ethanol (which increases virulence in *A. baumannii* infection of *Dictyostelium discoideum* and *Caenorhabditis elegans* (30)). Total RNA was isolated from the 16 conditions, pooled, and used as a single sample.

To enrich for primary transcripts, an aliquot from the pooled sample was digested with Terminator Exonuclease (TEX) (10). Over 20 million mapped sequencing reads were analyzed with TSSpredator software (21) and manually inspected with Integrated Genome Browser (IGB) and Jbrowse (17,18) to define the genomic location of 3731 TSS (Figure 1). The TSS of ACX60_RS00325 encoding a putative 4-hydroxyphenylpyruvate dioxygenase was independently confirmed by 5′ RACE and agreed with the TSS determined by dRNA-seq (Supplementary Figure S1). In addition, three biological replicates of RNA isolated from OD_{600} 2.0 (early stationary phase (ESP)) yielded over 6.7 million mapped reads for each of the ESP biological replicates and the >20 million mapped reads for the remaining aliquot from the pooled RNA sample (i.e. the aliquot not treated with TEX) provided sufficient depth to cover the bacterial transcriptome (31).

TSS were categorized according to their locations relative to coding sequences (Figure 2A). Of 3731 TSS, 1079 (∼29%) were primary and 153 (∼4%) were secondary TSS (Figure 2B and Supplementary Table S2). Manual curation of the TSS predictions determined that five TSS had a 5′ UTR longer than 400 nt (Figure 2C). It is likely that these cases represent unusually long 5′ UTRs; however, it is possible that these regions encode small open reading frames missed during automated gene annotation (Figure 2C). About 18% (679) of transcripts were initiated from inside of coding regions (i.e. internal TSS). An internal TSS can drive expression of downstream genes, e.g. the promoter of DNA gyrase B-encoding gene (*gyrB*) lies within the ORF located upstream encoding DNA recombination protein RecF. The biological role of internal promoters that do not drive the expression of a downstream gene is unclear, however, a subset initiates the expression of small RNAs located at the 3′ end of coding genes (see below). TSSpredator predicted that almost half (∼47%, 1764/3731) of the identified TSS are located antisense of coding regions. Manual inspection revealed that the large majority of antisense TSS produce very short (<100 nt) and low-copy transcripts. The function of these short antisense transcripts is debated and a portion might be considered as non-functional transcripts that are initiated at promoter-like sequences (32,33). However, an increasing number of studies suggest that pervasive transcription (including short antisense transcripts) exhibit biological roles (34). The ∼1.5% (56/3731) of TSS that do not have a clear association with an annotated genomic feature were categorized as orphan TSS.

A. baumannii promoter architecture

To initiate transcription, a sigma factor directs binding of RNA polymerase to DNA within 50 nt upstream of a TSS (35). We determined the consensus promoter structure upstream of the 3731 TSS using unbiased motif searching to detect TSS-proximal and TSS-distal motifs corresponding to the −10 and −35 locations of sigma factor binding sites. Because the spacing between −10 and −35 binding sites differs between promoters, we searched for each motif separately; constraining a specific spacing between −10 and −35 elements prevents resolution of the weaker motifs located around the −35 position. MEME searching identified canonical RpoD (sigma 70) binding site motifs in both the −10 and −35 locations (Figure 2D), consistent

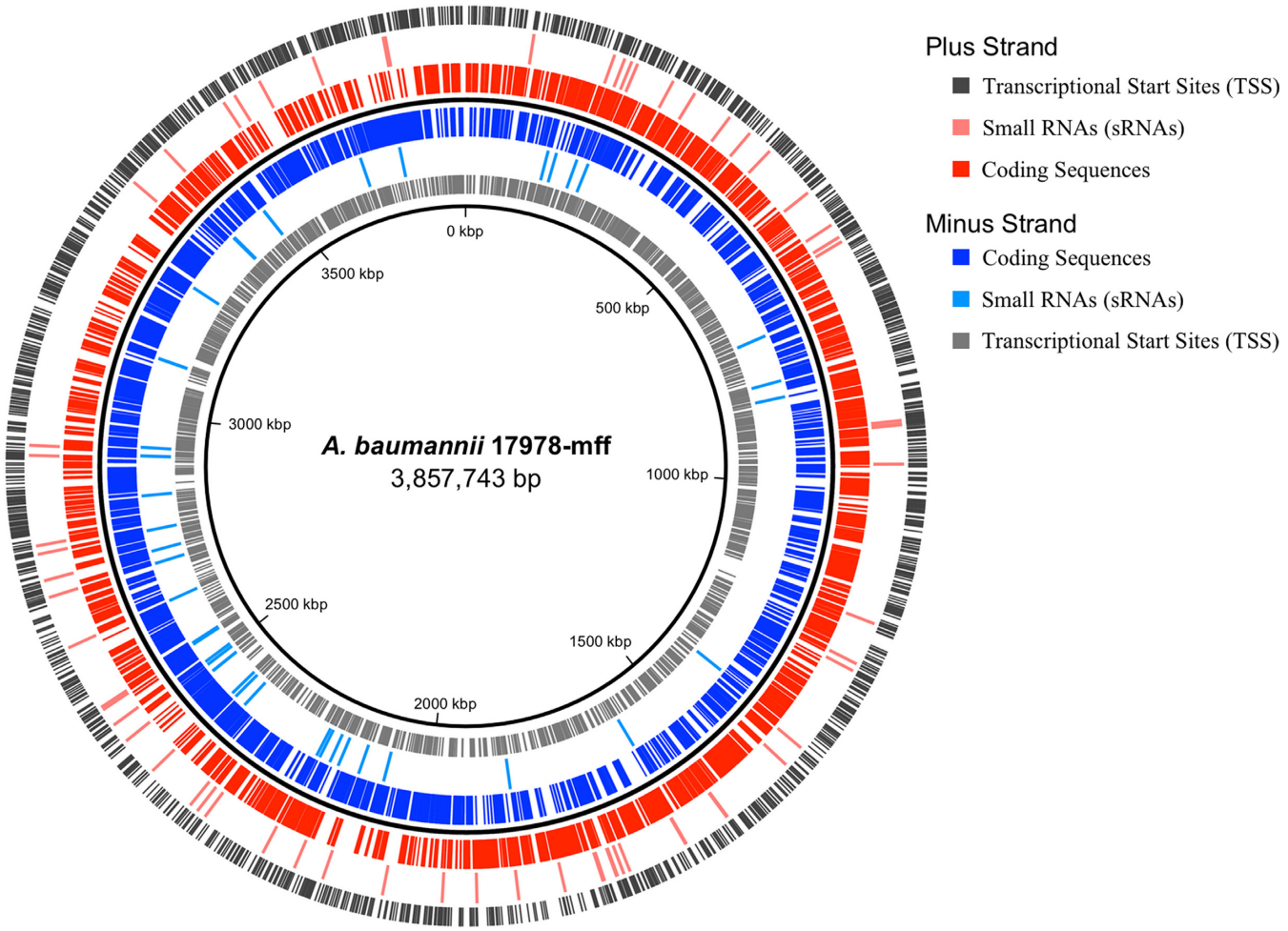

Figure 1. Chromosomal location of coding sequences, small RNAs and TSS of *A. baumannii* ATCC 17978-mff. Coding sequences are depicted in blue and red (plus and minus strand), small RNAs in light blue (plus strand) and light red (minus strand) and TSS in outer dark grey ring: TSS on the plus strand, inner light gray ring: TSS on the minus strand). The figure was created using Circa (OMGenomics, http://omgenomics.com/circa/).

with the expectation that RpoD is responsible for a large majority of transcription initiation in *A. baumannii*. Aligning all 3731 *A. baumannii* TSS revealed that adenine is the most common initiating nucleotide (A = 47%) (Figure 2C). The majority of transcripts initiate with a purine nucleotide triphosphate (ATP = 47%, GTP = 23%); these are the most abundant nucleotides and are the primary energy storage molecules, thus provide a mechanism to reduce transcription initiation when nucleotide and energy pools are depleted. Yet it is position +2 that has the strongest sequence bias (T = 57%). Pyrimidine nucleotides are less abundant in cells, and the preference for pyrimidine nucleotides at the −1 (72% C+T) and +2 (81% C+T) positions immediately flanking the TSS may represent a mechanism to focus transcription initiation at the purine-requiring position +1 (11). In other words, preference for pyrimidines at positions −1 and +2 arises because of selection against having purines at these positions.

UTR of mRNA perform multiple biological functions, including providing binding sites for ribosomes and the potential to fold into mRNA secondary structures that regulate transcription and RNA stability (36). The median length of 5′ UTR for primary TSS is 37 nt and secondary TSS is 100 nt (Figure 2C). Similar UTR analyses have not been performed for the *E. coli* transcriptome; the median length of 5′ UTR in *Salmonella* Typhimurium, another Gamma-proteobacterium, is 55 nt for primary TSS and 124 nt for secondary TSS (11).

Identification of *A. baumannii* ATCC 17978 small RNAs

Small, regulatory RNAs are a class of post-transcriptional regulators that modulate gene expression of many cellular processes (37,38). Functions have been determined for some sRNAs in *Enterobacteriaceae* (e.g. *E. coli*, *Salmonella* Typhimurium), but no sRNA functions have been experimentally determined in *A. baumannii* (5). Two previous studies used bioinformatic and experimental approaches to locate small RNAs in *A. baumannii*. In *A. baumannii* MTCC 1425 (ATCC 15308), 31 sRNAs were predicted bioinformatically, of which three of which were verified by Northern blotting (39). In *A. baumannii* AB5075, RNA-seq analysis of exponential growth in lysogeny broth (LB) identified 78 sRNAs, six of which were verified by Northern blotting (40). Here, we employed dRNA-seq on pooled growth con-

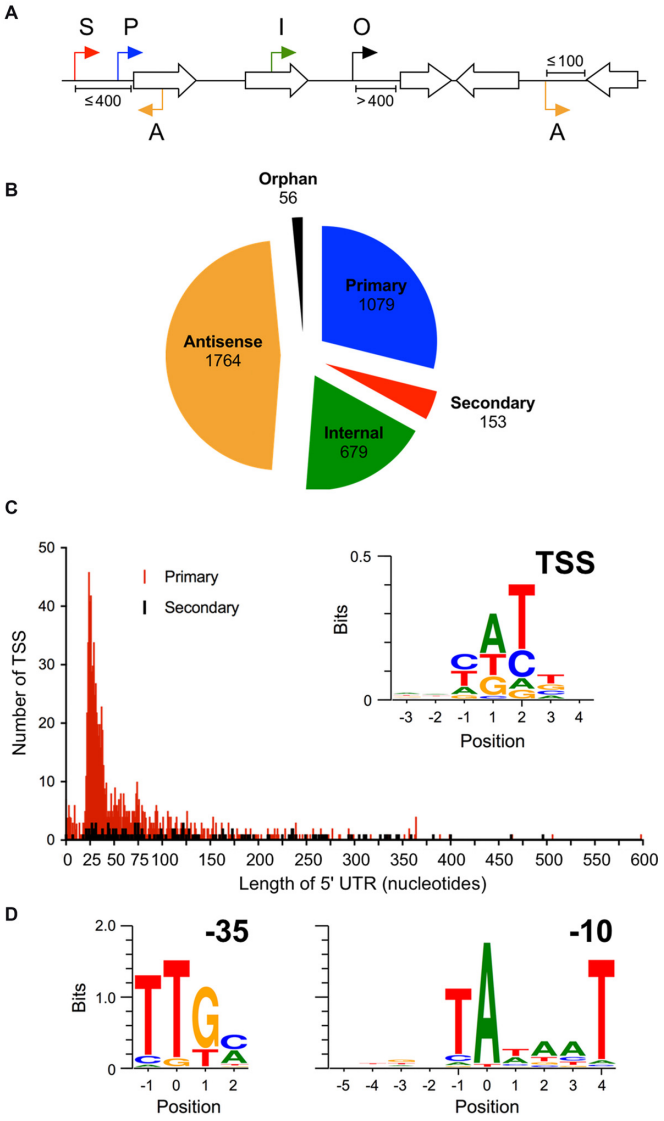

Figure 2. Characterization of TSS. **(A)** Schematic explaining TSS categories. P: Primary TSS, S: Secondary TSS, I: Internal TSS, A: Antisense TSS, O: Orphan TSS. **(B)** Pie chart showing the number of TSS per category. **(C)** Histogram showing the number and length of 5′ UTRs of primary (red) and secondary (black) TSS. The inset illustrates the frequency of occurrence of nucleotides around the TSS. **(D)** Meme-derived motifs showing −35 and −10 region of *A. baumannii* ATCC 17978 promoters.

ditions for *de novo* detection of sRNA candidates; pooled RNA samples coupled with the high resolution determination of TSS has been shown to identify a greater number of sRNA per genome compared to traditional methods (12). Using the search criteria described in Material and Methods, sRNAs could occur within intergenic regions, antisense to known coding regions, or within the 3′ end of mRNA. dRNA-seq provided the necessary resolution to detect TSS within the 3′ end of coding genes. We identified a total of 110 candidate sRNAs expressed by *A. baumannii* in the pooled growth condition (Supplementary Table S3). As an example of sRNA annotation, mapped sequence reads of eight sRNAs is depicted in Figure 3A. The majority (74/110; 67%) of sRNAs were in intergenic regions. The 3′ regions of cod-

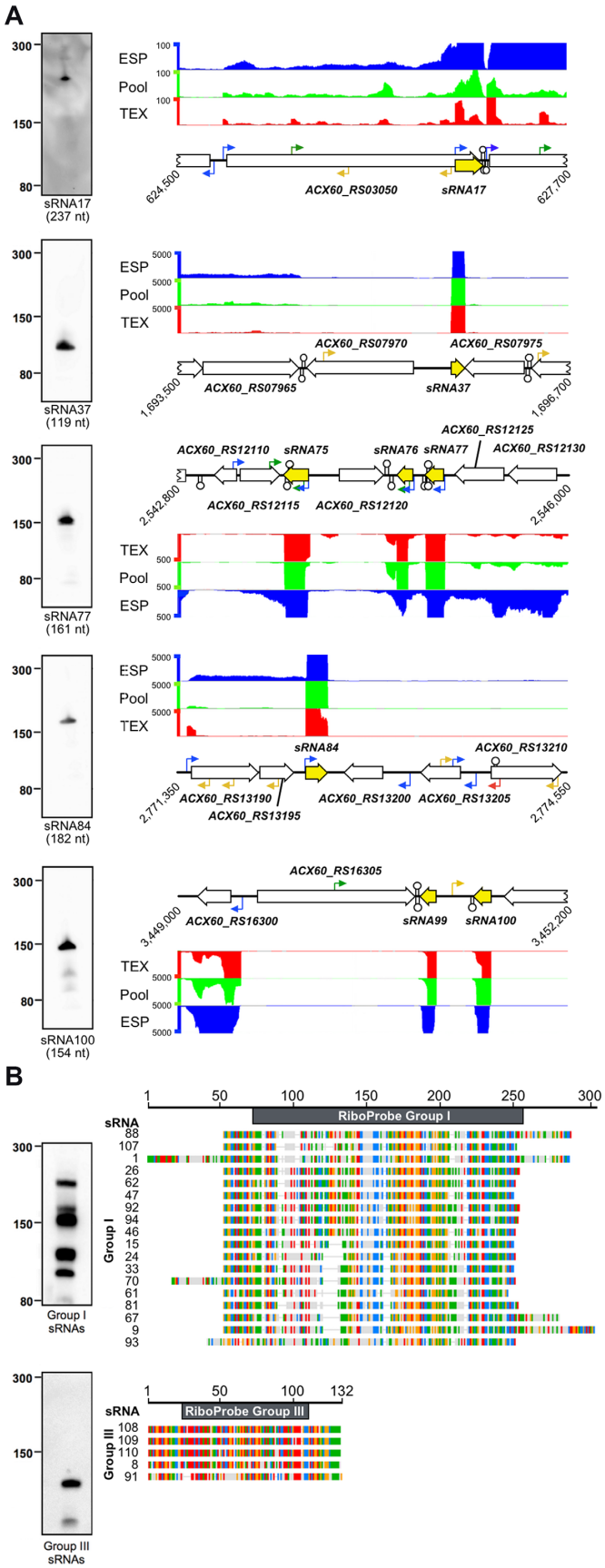

Figure 3. sRNA in *A. baumannii* ATCC 17978. (**A**) Normalized, mapped sequence reads from RNA-seq show the expression of sRNAs 17, 37, 75,

ing genes are increasingly recognized as genomic locations that can harbor sRNA genes (6,41,42). In *A. baumannii*, we identified 22 sRNAs that mapped to the 3′ regions of coding genes, all of which possess their own promoters located within the upstream coding gene. We anticipate that there will be additional regulatory sRNAs produced by endonucleolytic processing of an mRNA, as observed in other bacteria (42). However, additional experiments are required to annotate such sRNAs effectively (42). Only a small number (14/110; 13%) of sRNAs were located antisense of coding genes.

We used Northern blots to validate sRNA annotations (Figure 3). Sequence-specific riboprobes were designed to hybridize to two families of homologous sRNAs and five randomly selected unique sRNA candidates, including one sRNA (sRNA17) located in the 3′ region of ACX60_RS03050, a predicted TonB-dependent receptor protein. Eighteen of the 110 sRNA candidates were homologs (i.e. present as 18 copies with highly similar nucleotide sequence), which we classified as 'group I sRNAs' (Figure 3B). Gene duplications are common amongst sRNA species and may benefit the bacterium by allowing for rapid evolution and diversification of gene regulation (37). The transcriptomic data suggested a variable length of the group I sRNAs and Northern blotting with a riboprobe hybridizing to the homologous region of group I sRNAs displayed multiple bands between 100–250 nt in length. The group I family of *A. baumannii* ATCC 17978 sRNAs corresponds to the 'C4-similar' group in *A. baumannii* AB5075, reported previously to share regions of homology with bacteriophage P1 and P7 (40). Two of the group I *A. baumannii* ATCC 17978 sRNAs contained a 5′ region with low sequence homology; the diversity in this region may provide these particular sRNAs with additional species-specific functions (Figure 3B).

We next considered orthologs of sRNA that have been characterized in model species like *E. coli*. sRNA37 (119 nt) is predicted to be the 4.5S RNA of the signal recognition particle that is involved in membrane protein targeting. sRNA84 (182 nt) is predicted to be the 6S RNA that can bind and inhibit RNA polymerase in *E. coli* (5).

The RNA binding proteins Hfq, CsrA or ProQ coordinate binding of sRNAs to target mRNAs in *Enterobacteriaceae* (43–45). Only Hfq has been studied functionally in *Acinetobacter* spp. (46,47) and it possesses an unusually long, glycine-rich C-terminus that could alter Hfq function compared to what has been observed in model species (47). Thus, post-transcriptional regulation by Hfq and other RNA-binding proteins should be explored in *Acinetobacter* species.

Conservation of *Acinetobacter* small RNAs

A gene conservation analysis was carried out by comparing the nucleotide sequence identity of the sRNAs identified in 17978-mff with other bacterial genomes. The search approach started by comparing members of the same species, then was expanded to representative members of the genus, and finally among other members of the order Pseudomonadales. The suite of 27 genomes contained fifteen *A. baumannii* strains, seven species in the genus *Acinetobacter*, and five more distantly related members of the order Pseudomonadales (Figure 4). The most highly conserved sRNA across all species were 4.5S RNA (sRNA37), 6S RNA (sRNA84) and to a lesser extent tmRNA (sRNA89), but the level of conservation drops rapidly outside of the genus. The conservation of *A. baumannii* sRNAs was much higher in the opportunistic pathogens *A. pittii* and *A. nosocomialis* showing a mean sequence identity across all 110 sRNAs of ∼87% for *A. pittii* and ∼84% for *A. nosocomialis* compared to other *Acinetobacter* species. Environmental, non-pathogenic *Acinetobacter* species had lower mean sequence identity. Using a 70% sequence identity cutoff, five sRNAs are present only in *A. baumannii* 17978 (sRNA11, sRNA23, sRNA52, sRNA82, and sRNA83). Searching for sRNA homologs in other members of the order Pseudomonadales revealed that only a very small number of sRNA with sequence identity >70% are found outside of the genus *Acinetobacter*. A broader search revealed that no *A. baumannii* sRNA are present in *E. coli* or *Salmonella* Typhimurium. sRNAs conserved in *A. baumannii* sRNA but absent from other species may have evolved for roles in *A. baumannii* virulence or antibiotic resistance, making these good targets for future studies. Unfortunately, the biological functions of *Acinetobacter* sRNAs are hard to predict due to the low level of sequence conservation between *Acinetobacter* sRNAs and well-characterized sRNAs from relatively closely-related *Pseudomonas* species.

Functional genomics for the study of virulence and antimicrobial resistance in *A. baumannii*

A. baumannii is responsible for an increasing number of hospitalized cases of pneumonia leading to death, which has fueled efforts to identify genes that are important for virulence, host colonization and antimicrobial resistance. In a mouse model of *A. baumannii* pneumonia, genome-wide transposon mutagenesis followed by DNA sequencing (insertion sequencing) identified 157 genes associated with *A. baumannii* persistence in the lung confirming the importance of known virulence genes and identifying several genes with no previous connection to *A. baumannii* infection (48). Our dataset builds upon this analysis by offering detailed molecular insights into the transcriptional architecture of important *A. baumannii* virulence factors. This dataset is useful to the study of other *A. baumannii* strains because many promoter regions are highly conserved between clinically-relevant strains. For example, the TSS and promoter sequences for the primary virulence factor *ompA*

←

76, 77, 84, 99 and 100 (yellow arrows). Curved arrows depict TSS identified in this study and lollipop structures are predicted rho-independent terminators. Northern blotting of selected sRNAs are shown to the right. RNA was isolated from ESP and five μg of total RNA was loaded per lane. The sRNA sizes below the individual blots have been predicted from dRNA-seq data. (**B**) Sequence alignment of Group I and Group III sRNAs created with the Geneious Software (v. 8.1.8); colored bases indicate conservation in at least 50% of aligned sequences (A, red; C, blue; G, yellow; T, green). The riboprobes used in Northern blotting are depicted as black bars atop the sRNA alignments.

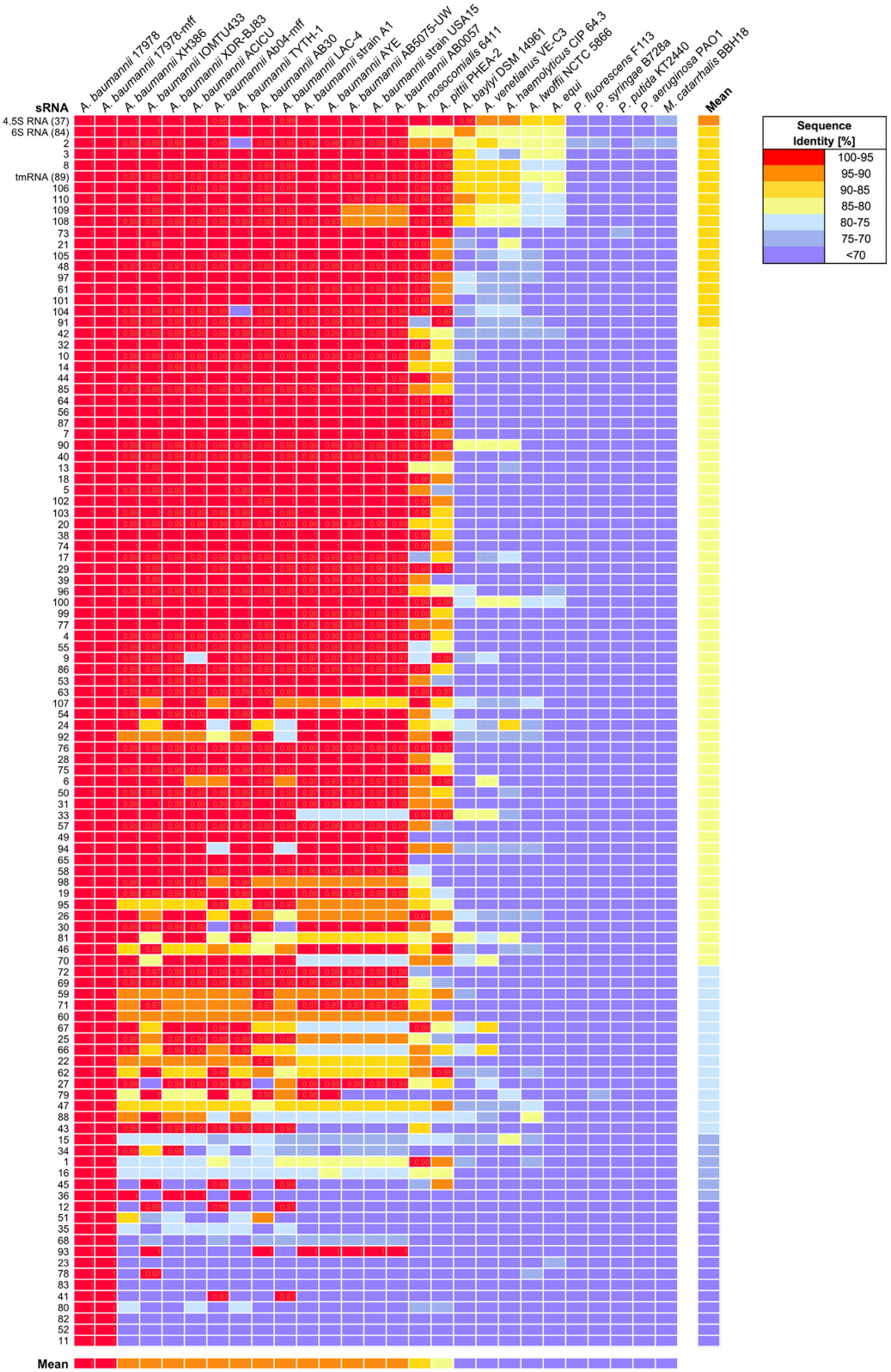

Figure 4. sRNA conservation in representative members of the order Pseudomonadales. Genomes of multiple *Acinetobacter* species, *Pseudomonas* species, and *Moraxella catarrhalis* were compared using GLSEARCH. The colour scale shows the percentage sequence identity of the 110 sRNAs compared to the reference sequence from *A. baumannii* ATCC 17978.

are conserved across *A. baumannii* strains, suggesting the same TSS is used by all members of the species (Supplementary Figure S2). Here, we provide examples of how AcinetoCom can be used by researchers to evaluate transcriptional features of both well-characterized and novel virulence factors, and discuss the importance of *in vitro* growth conditions in the study of virulence gene expression (Supplementary Table S4).

Regulation of zinc acquisition and the Znu *ABC transporter.* Metal acquisition genes are a critical component in *A. baumannii* virulence as they are required to wrest essential co-factors from host chelators (5,49,50). Zinc limitation has been demonstrated as a central feature in controlling bacterial replication in the lung and dissemination to systemic sites in the murine model of *A. baumannii* pneumonia (49,51). In *A. baumannii*, the Zur (zinc uptake regulator, ACX60_RS17350) transcriptional regulator is responsible for mediating the expression of several zinc-associated functions, including the repression of an ABC family zinc transporter encoded by *znuABC*. In *A. baumannii* ATCC 17978, the *zur* gene is co-transcribed as part of an operon with *znuCB*, which encode the cognate ATPase and permease protein of the ABC transporter (49). The third component, *znuA*, is found on the opposite DNA strand and encodes a substrate-binding protein (49). During growth in zinc-replete conditions, the Zur protein binds to a 19-bp operator site located 30 nucleotides upstream from the *znuA* translation start site and represses the expression of both *znuA* and the *zurznuCB* operon (49,51).

TSSpredator identified a total of 8 TSS within the chromosomal region that includes both the *znuA* gene and *zurznuCB* operon (Figure 5A). Two of the TSS were located 29 and 93 nucleotides upstream of the *znuA* ORF. While both TSS were annotated as antisense to the *zur* gene, their location within the intergenic region also make them prime candidates as primary or secondary TSS to *znuA*. The *zurznuCB* operon was expressed in our test conditions. Although a potential TSS could be observed at position (3 647 395) in the ESP and Pool samples, it was not enriched in the TEX sample relative to the Pool RNA sample. This loss of a TSS-like peak in the TEX sample suggests that the TSS could be a substrate of a cellular 5′ pyrophosphohydrolase (52). When this enzyme converts 5′ triphosphates into monophosphates, TEX will digest this unprotected TSS. Based on the above predictions, the TSS for *znuA* or *zurznuCB* are found on either side of the Zur-binding site and may represent an important regulatory feature for Zur-based transcription repression (49,51). An additional TSS was identified within the *znuC* ORF, located 239 nucleotides upstream of *znuB*. To our knowledge, this TSS has not been previously identified in the well-characterized *zurznuCB* operon and suggests the potential for transcription of *znuB* independently from other members within the operon. Such a format of expression may be a mechanism for cells to accommodate modest increases in the intracellular level of zinc while avoiding simultaneous increases in the Zur protein. Further, there are no reports of a Zur box associated with the region surrounding this internal TSS. A Rho-independent transcriptional terminator is also present in this region, located within the *znuB* ORF or 113 nucleotides downstream of *znuC*. Several additional internal TSS were also identified within the *znuA* gene, but did not demonstrate a clear association with downstream genes or with an sRNA transcript. The remaining TSS within the re-

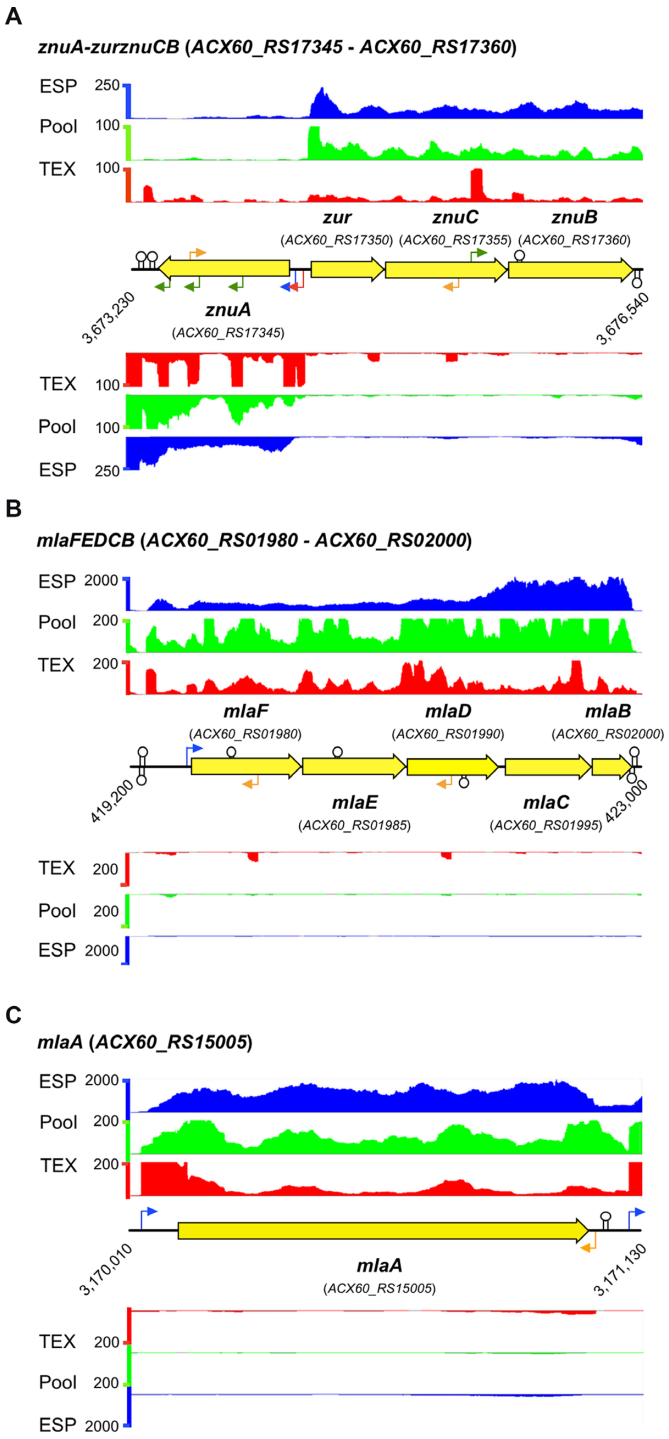

Figure 5. RNA-seq analysis of *znu* and *mla* virulence operon gene expression. Mapped, normalized RNA-seq reads illustrate the quantitative measure of expression. Right-angle arrows indicate TSS, which are colour-coded to correspond with the TSS categories described in Figure 2. The lollipop structures represent predicted Rho-independent transcriptional terminators.

gion were annotated as antisense TSS and contribute to the overall theme of pervasive low-level antisense transcription within the *A. baumannii* transcriptome.

The membrane lipid asymmetry (Mla) transport system. Several of the genes responsible for *A. baumannii* persistence in the mouse pneumonia model were identified as belonging to efflux pump systems (48). The authors highlighted the Mla ATP-binding cassette (ABC) transport system because this system was annotated as conferring a toluene tolerance phenotype (53), raising the question of why resistance to organic solvents may be important during infection of a mammalian host. However, recent studies have since uncovered a central role for Mla-mediated transport in maintaining the integrity of the outer membrane of Gram-negative bacteria (54,55). Wang *et al*. reported a 15-fold decrease in *in vivo* persistence of mutants lacking *mlaA* (48), which correlates with roles for the Mla transport system in iron limitation and outer membrane vesicle formation as well as resistance to antibiotics such as doripenem and colistin (56–58).

Our transcriptomic data reveal that genes encoding the Mla ABC transporter components and periplasmic binding protein are co-transcribed in the *mlaFEDCB* operon (Figure 5B). Similar to the *zurznuCB* operon, TSSpredator did not call a TSS upstream of this operon because of a lack of enrichment compared to the Pool sample, but manual inspection of the mapped reads suggest a single TSS located 29 nt upstream of *mlaF* at position 419,650. We noted greater transcript abundance of *mlaDCB* (most notably *mlaCB*) compared to *mlaFE* in ESP, an expression pattern that was also observed for an LPS-deficient mutant of *A. baumannii* strain 19606 (56). As there is no additional promoter within the operon, this suggests that the *mlaDCB* portion of the transcript may turnover more slowly or is protected from degradation resulting in elevated production of the periplasmic substrate binding domain MlaC. A Rho-independent terminator was identified downstream of the operon and provides a potential 3′ border for the transcript; however, multiple rho-independent terminators were also identified within the operon, with two terminators present early in the *mlaF* and *mlaE* ORFs. Like *E. coli* and other Gram-negative bacteria, the *A. baumannii mlaA* homolog is found at a separate location on the chromosome (Figure 5C) and we identified a single TSS for *mlaA*, located 74 nt upstream of the start codon. An additional antisense TSS was also identified, located opposite of the 3′ end of the *mlaA* ORF. Both the *mlaFEDCB* and *mlaA* loci were expressed during ESP, suggesting that this growth condition could be used for further investigation of the transport system.

Chloramphenicol resistance is regulated by transcription initiation. We discovered that *A. baumannii* ATCC 17978 cultured in M9 medium loses resistance to chloramphenicol (Figure 6). All *A. baumannii* strains contain the chromosomally-encoded efflux pump CraA (ACX60_RS01760), for chloramphenicol resistance *Acinetobacter*, also called MdfA. Efflux by CraA appears to be highly specific to chloramphenicol, conferring a minimum inhibitory concentration >256 μg mL^{-1} chloramphenicol (59). Inhibition of CraA in *A. baumannii* strain 19606 increases sensitivity by 32-fold while deletion of *craA* increases sensitivity by 128-fold, respectively (59). Expression of *craA* is highly consistent between strains of multi-drug resistant *A. baumannii* (60), but it is not known if this expression is constitutive in nature (61). In *A. baylyi*, a point mutation 12 bp upstream of the *craA* start codon caused increased stability of the *craA* mRNA resulting in higher *craA* expression and increased resistance to chloramphenicol (62).

We used dRNA-seq and quantitative PCR to examine the promoter architecture and regulation of *craA* in *A. baumannii* ATCC 17978, and tested whether loss of chloramphenicol resistance is coupled to altered expression of *craA* (Figure 6A). dRNA-seq revealed two promoters at the *craA* gene, the gene-proximal TSS-1 promoter (position 367,680, Supplementary Table S2) and the gene distal TSS-2 promoter (position 367,564, Supplementary Table S2). Phylogenetic comparisons confirmed that these promoter elements are conserved across *A. baumannii* strains (Supplementary Figure S3). To examine how *craA* expression is regulated in response to growth conditions, we used qPCR to differentiate transcripts originating at TSS-1 from TSS-2. Because TSS-1 is contained within TSS-2 transcripts, TSS-1 transcripts were calculated by subtracting TSS-2 transcripts from total *craA* transcripts. During steady-state rapid growth (exponential phase) in nutrient-rich L-broth, 92% of *craA* transcription originates at TSS-1 (Figure 6A). Conversely, in the nutrient-poor medium M9 plus pyruvate, TSS-1 activity was undetectable and all transcription was driven by TSS-2. Next, we tested how the two promoters responded to nutrient downshift. Within four hours of transferring exponentially-growing cells from L-broth to M9 plus pyruvate, TSS-1 was down-regulated by 50-fold, whereas TSS-2 was down-regulated only 1.4-fold (Figure 6B). Therefore, the promoter driving TSS-1 is highly responsive to nutritional quality of the growth medium. Over the following days, both promoters continued to decline in activity. TSS-1 has a poor match to the RpoD −35 consensus, suggesting that protein transcription factors control TSS-1 by recruiting RNAP to the promoter. The TSS-2 promoter contains an archetypical −35 sequence, suggesting that RNAP can bind this promoter without assistance from an activator protein, which could explain the consistent expression of TSS-2 in L-broth and M9 medium.

We hypothesized that down-regulation of *craA* in M9 medium would result in a chloramphenicol-sensitive phenotype akin to that of a *craA* mutant strain. Thus, we evaluated the proportion of resistant and sensitive *A. baumannii* cells in liquid cultures. During exponential growth in rich medium (L-broth), all cells were resistant to chloramphenicol (Figure 6B). All cells remained resistant at 4 h after transfer to M9 medium, but 24 h after transfer to minimal media, 50% of cells were susceptible. Cell viability was high after 96 h in M9 medium, but chloramphenicol resistance had declined by >3000-fold (Figure 6B). Taken together, these results suggest that antibiotic resistance is conditional, especially when cells are instantly deprived of amino acids upon transfer from Lennox medium to M9 plus pyruvate medium. Although chloramphenicol resistance is ubiquitous in *A. baumannii* isolates due to drug efflux by CraA,

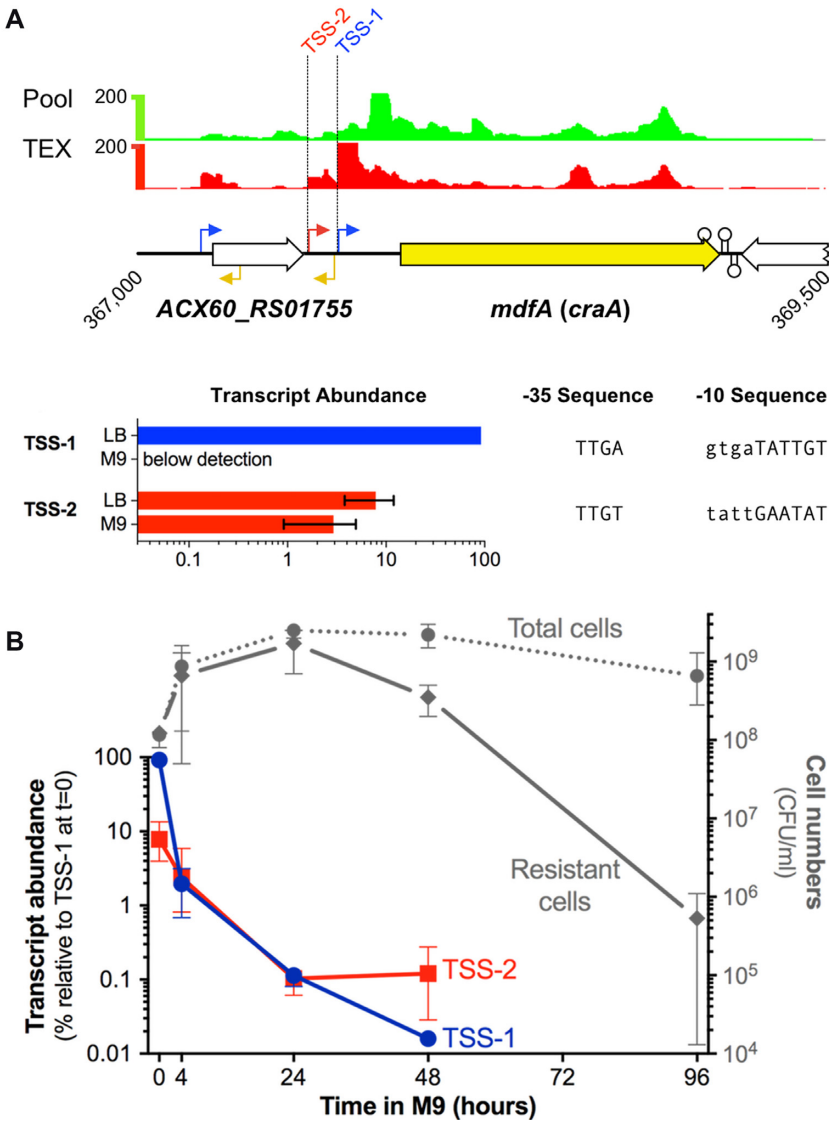

Figure 6. Elucidation of transcriptional control of chloramphenicol resistance. (**A**) Normalized, mapped sequence reads from dRNA-seq of the RNA pool (upper panel). Right-angle arrows indicate the two TSS identified in the promoter region of the chloramphenicol efflux pump gene, *craA*, also called multidrug efflux pump, *mdfA*. The lollipop structure represents a predicted rho-independent transcriptional terminator. Transcript abundance was quantified for TSS-1 or TSS-2 and expressed relative to total transcript abundance in cells growing exponentially in LB medium, with predicted −10 and −35 RNAP binding sites. (**B**) Growth experiment of *A. baumannii* in M9 over 96 hours. At the indicated time points, *A. baumannii* cells were plated on LB agar (Total cells) or LB + chloramphenicol (resistant cells). Transcript abundance of *craA* mRNA originating from TSS-1 or TSS-1+2 measured by qPCR at 0, 4, 24 and 48 h.

we have discovered that *craA* expression—and thus chloramphenicol resistance—is conditional on nutritional quality of the environment. This lack of endogenous activation or repression of drug resistance presents a potential target for the effective treatment of multi-drug resistant infections with an inexpensive and widely available antibiotic.

CONCLUSION

As an emerging pathogen in the 'omics' age, *A. baumannii* pathobiology is defined largely by high-throughput technologies that can guide molecular studies of pathogenicity mechanisms and antimicrobial resistance. We have conducted the first dRNA-seq analysis of the model strain *A. baumannii* ATCC 17978 to identify several thousand TSS at single nucleotide resolution, and generated a comprehensive map of the transcriptome that includes 110 sRNAs. Although 3731 TSS is the largest and most precise dataset yet for *Acinetobacter*, it is important to note that computational identification of TSS can overlook true sites. TSS are only called where a sharp increase in read depth in the TEX-treated sample exceeds the normalized read depth in the Pool sample. Overall, we identified an average of 5.1 sense strand TSS/10 kb in *A. baumannii* ATCC 17978, which is similar but fewer than the 7.0 sense strand TSS/10 kb identified in *S.* Typhimurium 4/74 (12). Because manual curation of *S.* Typhimurium 4/74 identified more TSS per bp, we suspect the TSSpredator program used here did not identify

all TSS. Thus, scientists using AcinetoCom are encouraged to examine the RNA-seq read depth at their gene(s) of interest. A sharp increase in read depth in the TEX track alone can be highly suggestive of a TSS. Thus, investigators are advised to scrutinize cases where there is high expression in the ESP tracks but no TSS is called in the TEX track.

A growing body of evidence suggests a positive relationship between conditions that slow bacterial growth and the expression of virulence factors. For notable pathogens such as *Legionella*, *Yersinia* and *Salmonella*, key virulence traits are induced during the early stationary phase in laboratory culture (11,63–66). Expression of virulence determinants in standard laboratory conditions has permitted the study of gene function and characterization of the regulatory networks that control virulence gene expression in other model pathogens (67). It was fortuitous to discover that *A. baumannii* expresses key pathogenicity genes in standard laboratory conditions, including the three loci identified in the mouse model of pneumonia (5,48) highlighted in Figure 5. Similarly, simple laboratory conditions revealed an environmental dimension to the control of drug resistance in *A. baumannii*. Although diagnostic techniques that test for the presence of antibiotic resistance genes can predict resistance, our finding of chloramphenicol sensitivity in a species that is considered highly chloramphenicol resistant illustrates the importance of characterizing gene expression and gene regulatory mechanisms. Reduced chloramphenicol efflux due to rapid down-regulation of *craA* expression presents two intriguing leads for combating this ubiquitous resistance mechanism in *A. baumannii*. First, characterization of the regulatory mechanism and identification of the environmental cues that stimulate or repress *craA* expression will raise the potential to predict stages of infection and locations in the host that *A. baumannii* may be sensitive to chloramphenicol. Second, elucidation of the transcription factors controlling *craA* may reveal additional drug targets that could be targeted synergistically. This could enhance the effectiveness of a widely available and inexpensive antibiotic that is being used effectively in the treatment of other multi-drug resistant infections.

DATA AVAILABILITY

The raw data and normalized mapped reads are available from the Gene Expression Omnibus (GEO) at accession no: GSE103244. The AcinetoCom database can be accessed under http://bioinf.gen.tcd.ie/acinetocom/.

SUPPLEMENTARY DATA

Supplementary Data are available at NAR Online.

FUNDING

Saskatchewan Health Research Foundation [Establishment grant 2867 to A.D.S.C.]; Natural Sciences and Engineering Research Council of Canada [Discovery grant RGPIN-435784-2013 to A.D.S.C.]; Saskatchewan Health Research Foundation [3866 to K.D.M.]; Irish Research Council Government of Ireland Postdoctoral Fellowship [GOIPD/2016/292 to A.A.M.C.L.]. Funding for open access charge: University of Regina Research Office.

Conflict of interest statement. None declared.

REFERENCES

1. World Health Organization. (2017) *Global Priority List of Antibiotic-Resistant Bacteria to Guide Research, Discovery, and Development of New Antibiotics*. World Health Organization, Geneva.
2. Tacconelli,E., Carrara,E., Savoldi,A., Harbarth,S., Mendelson,M., Monnet,D.L., Pulcini,C., Kahlmeter,G., Kluytmans,J., Carmeli,Y. *et al.* (2018) Discovery, research, and development of new antibiotics: the WHO priority list of antibiotic-resistant bacteria and tuberculosis. *Lancet Infect. Dis.*, **18**, 318–327.
3. Spellberg,B. and Rex,J.H. (2013) The value of single-pathogen antibacterial agents. *Nat. Rev. Drug Discov.*, **12**, 963–963.
4. McConnell,M.J., Actis,L. and Pachón,J. (2013) *Acinetobacter baumannii*: human infections, factors contributing to pathogenesis and animal models. *FEMS Microbiol. Rev.*, **37**, 130–155.
5. Kröger,C., Kary,S.C., Schauer,K. and Cameron,A.D.S. (2016) Genetic regulation of virulence and antibiotic resistance in *Acinetobacter baumannii*. *Genes*, **8**, 12–19.
6. Colgan,A.M., Cameron,A.D. and Kröger,C. (2017) If it transcribes, we can sequence it: mining the complexities of host-pathogen-environment interactions using RNA-seq. *Curr. Opin. Microbiol.*, **36**, 37–46.
7. Saliba,A.-E., C Santos,S. and Vogel,J. (2017) New RNA-seq approaches for the study of bacterial pathogens. *Curr. Opin. Microbiol.*, **35**, 78–87.
8. Smith,M.G., Gianoulis,T.A., Pukatzki,S., Mekalanos,J.J., Ornston,L.N., Gerstein,M. and Snyder,M. (2007) New insights into *Acinetobacter baumannii* pathogenesis revealed by high-density pyrosequencing and transposon mutagenesis. *Genes Dev.*, **21**, 601–614.
9. Jacobs,A.C., Thompson,M.G., Black,C.C., Kessler,J.L., Clark,L.P., McQueary,C.N., Gancz,H.Y., Corey,B.W., Moon,J.K., Si,Y. *et al.* (2014) AB5075, a highly virulent isolate of *Acinetobacter baumannii*, as a model strain for the evaluation of pathogenesis and antimicrobial treatments. *mBio*, **5**, e01076-14.
10. Sharma,C.M., Hoffmann,S., Darfeuille,F., Reignier,J., Findeiß,S., Sittka,A., Chabas,S., Reiche,K., Hackermüller,J., Reinhardt,R. *et al.* (2010) The primary transcriptome of the major human pathogen *Helicobacter pylori*. *Nature*, **464**, 250–255.
11. Kröger,C., Dillon,S.C., Cameron,A.D.S., Papenfort,K., Sivasankaran,S.K., Hokamp,K., Chao,Y., Sittka,A., Hébrard,M., Händler,K. *et al.* (2012) The transcriptional landscape and small RNAs of *Salmonella enterica* serovar Typhimurium. *Proc. Natl. Acad. Sci. U.S.A.*, **109**, E1277–E1286.
12. Kröger,C., Colgan,A., Srikumar,S., Händler,K., Sivasankaran,S.K., Hammarlöf,D.L., Canals,R., Grissom,J.E., Conway,T., Hokamp,K. *et al.* (2013) An Infection-Relevant transcriptomic compendium for *Salmonella enterica* serovar Typhimurium. *Cell Host Microbe*, **14**, 683–695.
13. Weber,B.S., Ly,P.M., Irwin,J.N., Pukatzki,S. and Feldman,M.F. (2015) A multidrug resistance plasmid contains the molecular switch for type VI secretion in *Acinetobacter baumannii*. *Proc. Natl. Acad. Sci. U.S.A.*, **112**, 9442–9447.
14. Langmead,B. and Salzberg,S.L. (2012) Fast gapped-read alignment with Bowtie 2. *Nat. Methods*, **9**, 357–359.
15. Li,H., Handsaker,B., Wysoker,A., Fennell,T., Ruan,J., Homer,N., Marth,G., Abecasis,G., Durbin,R. and 1000 Genome Project Data Processing Subgroup (2009) The sequence Alignment/Map format and SAMtools. *Bioinformatics*, **25**, 2078–2079.
16. Afgan,E., Baker,D., van den Beek,M., Blankenberg,D., Bouvier,D., Čech,M., Chilton,J., Clements,D., Coraor,N., Eberhard,C. *et al.* (2016) The Galaxy platform for accessible, reproducible and collaborative biomedical analyses: 2016 update. *Nucleic Acids Res.*, **44**, W3–W10.
17. Nicol,J.W., Helt,G.A., Blanchard,S.G., Raja,A. and Loraine,A.E. (2009) The integrated genome browser: free software for distribution and exploration of genome-scale datasets. *Bioinformatics*, **25**, 2730–2731.
18. Skinner,M.E., Uzilov,A.V., Stein,L.D., Mungall,C.J. and Holmes,I.H. (2009) JBrowse: a next-generation genome browser. *Genome Res.*, **19**, 1630–1638.

19. Liao,Y., Smyth,G.K. and Shi,W. (2014) featureCounts: an efficient general purpose program for assigning sequence reads to genomic features. *Bioinformatics*, **30**, 923–930.
20. Li,B., Ruotti,V., Stewart,R.M., Thomson,J.A. and Dewey,C.N. (2009) RNA-Seq gene expression estimation with read mapping uncertainty. *Bioinformatics*, **26**, 493–500.
21. Dugar,G., Herbig,A., Förstner,K.U., Heidrich,N., Reinhardt,R., Nieselt,K. and Sharma,C.M. (2013) High-resolution transcriptome maps reveal Strain-Specific regulatory features of multiple *Campylobacter jejuni* isolates. *PLoS Genet.*, **9**, e1003495-15.
22. Vogel,J. (2003) RNomics in Escherichia coli detects new sRNA species and indicates parallel transcriptional output in bacteria. *Nucleic Acids Res.*, **31**, 6435–6443.
23. Bailey,T.L., Williams,N., Misleh,C. and Li,W.W. (2006) MEME: discovering and analyzing DNA and protein sequence motifs. *Nucleic Acids Res.*, **34**, W369–W373.
24. Crooks,G.E., Hon,G., Chandonia,J.-M. and Brenner,S.E. (2004) WebLogo: a sequence logo generator. *Genome Res.*, **14**, 1188–1190.
25. Naville,M., Ghuillot-Gaudeffroy,A., Marchais,A. and Gautheret,D. (2014) ARNold: A web tool for the prediction of Rho-independent transcription terminators. *RNA Biol.*, **8**, 11–13.
26. Pearson,W.R. (2001) *FASTA Search Programs*. John Wiley & Sons, Ltd, Chichester.
27. Tedin,K. and Bläsi,U. (1996) The RNA chain elongation rate of the lambda late mRNA is unaffected by high levels of ppGpp in the absence of amino acid starvation. *J. Biol. Chem.*, **271**, 17675–17686.
28. Eriksson,S., Lucchini,S., Thompson,A., Rhen,M. and Hinton,J.C.D. (2003) Unravelling the biology of macrophage infection by gene expression profiling of intracellular *Salmonella enterica*. *Mol. Microbiol.*, **47**, 103–118.
29. Cameron,A.D.S., Dillon,S.C., Kröger,C., Beran,L. and Dorman,C.J. (2017) Broad-scale redistribution of mRNA abundance and transcriptional machinery in response to growth rate in *Salmonella enterica* serovar Typhimurium. *Microb. Genom.* **3**, e000127.
30. Camarena,L., Bruno,V., Euskirchen,G., Poggio,S. and Snyder,M. (2010) Molecular mechanisms of ethanol-induced pathogenesis revealed by RNA-sequencing. *PLoS Pathog.*, **6**, e1000834.
31. Haas,B.J., Chin,M., Nusbaum,C., Birren,B.W. and Livny,J. (2012) How deep is deep enough for RNA-Seq profiling of bacterial transcriptomes? *BMC Genomics*, **13**, 734.
32. Raghavan,R., Sloan,D.B. and Ochman,H. (2012) Antisense transcription is pervasive but rarely conserved in enteric bacteria. *mBio*, **3**, e00156-12.
33. Lloréns-Rico,V., Cano,J., Kamminga,T., Gil,R., Latorre,A., Chen,W.-H., Bork,P., Glass,J.I., Serrano,L. and Lluch-Senar,M. (2016) Bacterial antisense RNAs are mainly the product of transcriptional noise. *Sci. Adv.*, **2**, e1501363.
34. Lybecker,M., Bilusic,I. and Raghavan,R. (2014) Pervasive transcription: detecting functional RNAs in bacteria. *Transcription*, **5**, e944039.
35. Davis,M.C., Kesthely,C.A., Franklin,E.A. and MacLellan,S.R. (2017) The essential activities of the bacterial sigma factor. *Can. J. Microbiol.*, **63**, 89–99.
36. Del Campo,C., Bartholomäus,A., Fedyunin,I. and Ignatova,Z. (2015) Secondary structure across the bacterial transcriptome reveals versatile roles in mRNA regulation and function. *PLoS Genet.*, **11**, e1005613.
37. Wagner,E.G.H. and Romby,P. (2015) Small RNAs in bacteria and archaea: who they are, what they do, and how they do it. *Adv. Genet.*, **90**, 133–208.
38. Nitzan,M., Rehani,R. and Margalit,H. (2017) Integration of bacterial small RNAs in regulatory networks. *Annu. Rev. Biophys.*, **46**, 131–148.
39. Sharma,R., Arya,S., Patil,S.D., Sharma,A., Jain,P.K., Navani,N.K. and Pathania,R. (2014) Identification of novel regulatory small RNAs in *Acinetobacter baumannii*. *PLoS One*, **9**, e93833-15.
40. Weiss,A., Broach,W.H., Lee,M.C. and Shaw,L.N. (2016) Towards the complete small RNome of *Acinetobacter baumannii*. *Microb. Genom.*, **2**, e000045.
41. Chao,Y., Papenfort,K., Reinhardt,R., Sharma,C.M. and Vogel,J. (2012) An atlas of Hfq-bound transcripts reveals 3′ UTRs as a genomic reservoir of regulatory small RNAs. *EMBO J.*, **31**, 4005–4019.
42. Miyakoshi,M., Chao,Y. and Vogel,J. (2015) Regulatory small RNAs from the 3′ regions of bacterial mRNAs. *Curr. Opin. Microbiol.*, **24**, 132–139.
43. Updegrove,T.B., Zhang,A. and Storz,G. (2016) Hfq: the flexible RNA matchmaker. *Curr. Opin. Microbiol.*, **30**, 133–138.
44. Vogel,J. and Luisi,B.F. (2011) Hfq and its constellation of RNA. *Nat. Rev. Microbiol.*, **9**, 578–589.
45. Smirnov,A., Wang,C., Drewry,L.L. and Vogel,J. (2017) Molecular mechanism of mRNA repression in trans by a ProQ-dependent small RNA. *EMBO J.*, **36**, 1029–1045.
46. Kuo,H.-Y., Chao,H.-H., Liao,P.-C., Hsu,L., Chang,K.-C., Tung,C.-H., Chen,C.-H. and Liou,M.-L. (2017) Functional characterization of *Acinetobacter baumannii* lacking the RNA chaperone Hfq. *Front. Microbiol.*, **8**, 97–12.
47. Schilling,D. and Gerischer,U. (2009) The *Acinetobacter baylyi* Hfq gene encodes a large protein with an unusual C terminus. *J. Bacteriol.*, **191**, 5553–5562.
48. Wang,N., Ozer,E.A., Mandel,M.J. and Hauser,A.R. (2014) Genome-wide identification of *Acinetobacter baumannii* genes necessary for persistence in the lung. *mBio*, **5**, e01163-14.
49. Hood,M.I., Mortensen,B.L., Moore,J.L., Zhang,Y., Kehl-Fie,T.E., Sugitani,N., Chazin,W.J., Caprioli,R.M. and Skaar,E.P. (2012) Identification of an *Acinetobacter baumannii* zinc acquisition system that facilitates resistance to Calprotectin-mediated zinc sequestration. *PLoS Pathog.*, **8**, e1003068-17.
50. Mortensen,B.L. and Skaar,E.P. (2013) The contribution of nutrient metal acquisition and metabolism to *Acinetobacter baumannii* survival within the host. *Front. Cell. Infect. Microbiol.*, **3**, 95.
51. Mortensen,B.L., Rathi,S., Chazin,W.J. and Skaar,E.P. (2014) Acinetobacter baumannii response to Host-Mediated zinc limitation requires the transcriptional regulator zur. *J. Bacteriol.*, **196**, 2616–2626.
52. Deana,A., Celesnik,H. and Belasco,J.G. (2008) The bacterial enzyme RppH triggers messenger RNA degradation by 5′ pyrophosphate removal. *Nature*, **451**, 355–358.
53. Kim,K., Lee,S., Lee,K. and Lim,D. (1998) Isolation and characterization of toluene-sensitive mutants from the toluene-resistant bacterium *Pseudomonas putida* GM73. *J. Bacteriol.*, **180**, 3692–3696.
54. Malinverni,J.C. and Silhavy,T.J. (2009) An ABC transport system that maintains lipid asymmetry in the gram-negative outer membrane. *Proc. Natl. Acad. Sci. U.S.A.*, **106**, 8009–8014.
55. Henderson,J.C., Zimmerman,S.M., Crofts,A.A., Boll,J.M., Kuhns,L.G., Herrera,C.M. and Trent,M.S. (2016) The power of asymmetry: architecture and assembly of the Gram-negative outer membrane lipid bilayer. *Annu. Rev. Microbiol.*, **70**, 255–278.
56. Henry,R., Vithanage,N., Harrison,P., Seemann,T., Coutts,S., Moffatt,J.H., Nation,R.L., Li,J., Harper,M., Adler,B. *et al.* (2012) Colistin-resistant, lipopolysaccharide-deficient *Acinetobacter baumannii* responds to lipopolysaccharide loss through increased expression of genes involved in the synthesis and transport of lipoproteins, phospholipids, and poly-β-1, 6-N-acetylglucosamine. *Antimicrob. Agents Chemother.*, **56**, 59–69.
57. Henry,R., Crane,B., Powell,D., Deveson Lucas,D., Li,Z., Aranda,J., Harrison,P., Nation,R.L., Adler,B., Harper,M. *et al.* (2015) The transcriptomic response of *Acinetobacter baumannii* to colistin and doripenem alone and in combination in an in vitropharmacokinetics/pharmacodynamics model. *J. Antimicrob. Chemother.*, **70**, 1303–1313.
58. Nhu,N.T.K., Riordan,D.W., Do Hoang Nhu,T., Thanh,D.P., Thwaites,G., Lan,N.P.H., Wren,B.W., Baker,S. and Stabler,R.A. (2016) The induction and identification of novel Colistin resistance mutations in *Acinetobacter baumannii* and their implications. *Nature Publishing Group*, **6**, 1–8.
59. Roca,I., Marti,S., Espinal,P., Martínez,P., Gibert,I. and Vila,J. (2009) CraA, a major facilitator superfamily efflux pump associated with chloramphenicol resistance in *Acinetobacter baumannii*. *Antimicrob. Agents Chemother.*, **53**, 4013–4014.
60. Lin,M.-F., Lin,Y.-Y., Tu,C.-C. and Lan,C.-Y. (2017) Distribution of different efflux pump genes in clinical isolates of multidrug-resistant *Acinetobacter baumannii* and their correlation with antimicrobial resistance. *J. Microbiol. Immunol. Infect.*, **50**, 224–231.

61. Coyne,S., Courvalin,P. and Périchon,B. (2011) Efflux-mediated antibiotic resistance in *Acinetobacter* spp. *Antimicrob. Agents Chemother.*, **55**, 947–953.
62. Brzoska,A.J., Hassan,K.A., de Leon,E.J., Paulsen,I.T. and Lewis,P.J. (2013) Single-step selection of drug resistant *Acinetobacter baylyi* ADP1 mutants reveals a functional redundancy in the recruitment of multidrug efflux systems. *PLoS One*, **8**, e56090.
63. Song,M., Kim,H.-J., Kim,E.Y., Shin,M., Lee,H.C., Hong,Y., Rhee,J.H., Yoon,H., Ryu,S., Lim,S. *et al.* (2004) ppGpp-dependent Stationary Phase Induction of Genes on *Salmonella* Pathogenicity Island 1. *J. Biol. Chem.*, **279**, 34183–34190.
64. Lee,C.A. and Falkow,S. (1990) The ability of *Salmonella* to enter mammalian cells is affected by bacterial growth state. *Proc. Natl. Acad. Sci. U.S.A.*, **87**, 4304–4308.
65. Pepe,J.C., Badger,J.L. and Miller,V.L. (1994) Growth phase and low pH affect the thermal regulation of the *Yersinia enterocolitica inv* gene. *Mol. Microbiol.*, **11**, 123–135.
66. Potrykus,K. and Cashel,M. (2008) (p)ppGpp: Still Magical? *Annu. Rev. Microbiol.*, **62**, 35–51.
67. Golubeva,Y.A., Sadik,A.Y., Ellermeier,J.R. and Slauch,J.M. (2012) Integrating global regulatory input into the *Salmonella* pathogenicity island 1 type III secretion system. *Genetics*, **190**, 79–90.